Integration of statistical spatial relations into Active Shape Model- Application to striatum segmentation in MRI

Saïd Ettaïeb
Research laboratory of signal, image and information Technology - University of Tunis El Manar-Tunisia
Rommana 1068, Tunis-B.P. n° 94, Tunisia
settaieb@gmail.com

Besma Mnassri
Higher Institute of Applied Sciences and Technology- University of Gafsa-Tunisia
Campus Universitaire-Sidi Ahmed Zarrouk – 2112, Gafsa, Tunisia
mnassribesma9@gmail.com

Kamel Hamrouni
Research laboratory of signal, image and information Technology - University of Tunis El Manar-Tunisia
Rommana 1068, Tunis-B.P. n° 94, Tunisia
kamel.hamrouni@enit.rnu.tn

ABSTRACT
This paper describes a new method based on Active Shape Model (ASM) and statistical spatial relations. It combines three types of a priori knowledge: the structures shapes, the distance and the angle variability between them. This knowledge is estimated during a training step. Then, the obtained models are used to guide the evolution of initial shapes during the segmentation step. The proposed method is applied to extract the striatum (Caudate nucleus and Putamen) on MR images of the brain. The obtained results are promising and show the performance of the proposed method.

Keywords
Statistical a prior knowledge, spatial relations, active shape model, MRI.

1. INTRODUCTION
Segmentation of medical images is a major issue and one of the most challenging topics. However, it is a hard task because of many factors. Indeed, medical images (scintigraphy, MRI, scanner...) are often characterized by low contrast, low resolution and the presence of noise. Moreover, the anatomical structures to be extracted are always complex and variable.

The conventional methods based only on the low-level characteristics of the image are not reliable, because the intensity of a pixel cannot guarantee an effective segmentation. To overcome these limits, many recent methods are proposed. They are taking into account high-level a priori knowledge, related to the anatomical structures during segmentation such as shape, texture, position, etc. These methods provide a powerful solution for a robust segmentation.

Among a priori knowledge, we can cite the spatial relations between structures which are often more stable than the appearance characteristics of the structures themselves. In this context, we proposed to integrate spatial relations into active shape model-ASM [Coo95]. The main idea is to exploit a priori knowledge of shape that exists in ASM and introduce new a priori knowledge about distance and angle variation between structures to be segment.

The aim is to define a new robust method well adapted for the segmentation of two structures, using three types of statistical a priori knowledge: the shape of each structure, the distance and the orientation variability between them. This knowledge is modeled during a training step, then, the obtained models are used to guide the segmentation process and guarantee the preservation of the distance and angle between shapes in the authorized intervals.

The proposed method is validated on a clinical application, where the problem consists in segmenting two structures of interest: caudate nucleus and putamen on MRI slices of the brain.

This paper is organized as follows: Section 2 reviews briefly related work. Section 3 is devoted to the integration of statistical spatial relations to guide the segmentation process. Finally, in Section 4, the proposed model is applied to localize two internal brain structures on MRI slices (caudate nucleus and putamen). The work is concluded in Section 5.

2. RELATED WORK
Many approaches for medical images segmentation have been developed over the years based on several techniques. First, conventional methods do not use any a priori knowledge and are fully based on low-level features mainly pixels intensities. The main drawback of these methods is being not robust enough because sometimes intensities in the same tissue are heterogeneous.

Such methods are highly sensitive to noise and produce satisfactory results unless if the contrast between structures is sufficiently marked.

To overcome these limits, new approaches based on a priori knowledge have been proposed. Among these methods, deformable models are widespread. They based on a priori knowledge of shape. They consist to put a curve close to the structure to be extracted that will be moved progressively to coincide to the edges of the region of interest while minimizing an energy term.

In this work, we are interested to these approaches because their principle is general and flexible making possible the integration a priori knowledge such as the spatial relations. Indeed, in literature, three basic types of spatial relations can exist between objects in an image: topological relations and metric relations who are in turn are partitioned to distance relations and direction relations [Hud08]. The topological relations represent the adjacency between structures. They show how an object partially or completely covers another object ("is adjacent to", "crosses ", "is included"). The distance relations describe the distance between structures ("close", "far", "to a distance of ") and the direction relations based on the six usual directions.

In the medical context, among the first remarkable work using spatial relations, we find that of Perchant [Per02]. He proposes a brain structures recognition procedure based on the matching of graphs: a graph derived from a reference image manually segmented by an expert and a graph of the image to be recognized. In [Gér00] Géraud et al. have proposed a sequential method of recognition of brain structures, where each structure is recognized through the structural information resulted from previously recognized structures. This information is generated from relations of distance and direction defined with respect to the already segmented structures.

However, in these works, spatial relations are always used in the recognition step, whereas the segmentation was achieved with conventional methods. To relieve these drawbacks, Colliot [Col04] invented a new methodology, which consists to directly introduce spatial relations in segmentation step. The segmentation is realized from the beginning in a region of interest defined by spatial relations. The spatial relations (direction, distance and adjacency) are represented by fuzzy sets and incorporated into the evolution equation of the active contour [Kas87a] as an external force. For the segmentation of a given structure, this force attracts the curve to the image areas where the spatial relationships are considered verified. The segmentation process is sequential. It is based on a graph that describes, in a hierarchical manner, the spatial relationships of brain anatomy.

Other recent works are published [Nem09, Fou10] where spatial relations are used either in the recognition step or in the segmentation step.

However, few works have opted for the integration of spatial knowledge into active shape models. One example is the work of Barhoumi et al. [Bar15] who proposed to incorporate a spatial relation of direction into an active shape model for the detection of Region of Interest in medical images. This spatial relation is modeled using fuzzy membership functions in order to model the uncertainty and the ambiguity of the spatial representation. In the same context, in [Jaa11], the authors have introduced a method that consists to add a spatial relation of distance to the active shape model. The a priori knowledge of spatial relation stems from a fuzzy logic modeling phase. In [Ett14], Ettaïeb et al. introduced a new statistical model of shape and spatial relation based on a priori knowledge of shape and a priori knowledge about the variation of a spatial distance relation.

The above methods have remarkably performed the medical images segmentation. Nevertheless, they have some known limitations. Indeed, the majority of them have combined a priori knowledge of shape which exists in the active shape model with one extra constraint either of distance or direction. In the present work, we propose to integrate two types of spatial relations into active shape model: spatial distance relation "A is at a distance of B" and spatial orientation relation based on the angle variation between two structures. These relations will be modeled statistically in a training step and used directly in the segmentation procedure.

3. ACTIVE SHAPE MODEL INTEGRATING STATISTICAL DISTANCE AND ORIENTATION MODELS

The basic idea of our contribution is to exploit a priori knowledge of shape that exists in ASM and introduce new a priori knowledge about distance and angle variation between the structures to be segment. This new knowledge will be estimated during a training step by two models: a distance model and an orientation model. These models will be then used to constrain the evolution of the shapes to the target structures and ensure maintenance of the distance and the angle between structures in the allowed intervals.

Thus, the proposed method requires two main steps:

• A training step, which aims to deduce, from a set of sample images, four basic models: a statistical shape model for each structure, a statistical distance model and a statistical orientation model.

• A segmentation step, based on the obtained models to guide the evolution of two initial shapes to the target structures.

Training Step

This step consists in collecting at first a set of samples of images reflecting the possible variations of two structures to be segmented. Then, we extract, from each image, the shape of each structure by placing a sufficient number of landmarks on the target contours. Considering that *n* and *m* are respectively the number of landmarks required to represent the details of the first and the second structure and *N* is the number of images in the training set, each structure can be represented by a matrix of points defined as follows:

$M_{st_1}(\boldsymbol{2n}, N) =$

$\boldsymbol{v_{11}}$	$\boldsymbol{v_{21}}$	$\boldsymbol{\ldots v_{i1} \ldots}$	$\boldsymbol{v_{N1}}$
x_{111}	x_{211}	….	x_{N11}
y_{111}	y_{211}	….	y_{N11}
⋮	⋮	….	⋮
x_{11n}	x_{21n}	….	x_{N1n}
y_{11n}	y_{21n}	….	y_{N1n}

$M_{str_2}(\boldsymbol{2m}, N) =$

$\boldsymbol{v_{12}}$	$\boldsymbol{v_{22}}$	$\boldsymbol{\ldots v_{i2} \ldots}$	$\boldsymbol{v_{N2}}$
x_{121}	x_{221}	….	x_{N21}
y_{121}	y_{221}	….	y_{N21}
⋮	⋮	….	⋮
x_{12m}	x_{22m}	….	x_{N2m}
y_{12m}	y_{22m}	….	y_{N2m}

With v_{ij} is the vector of points which models the structure *j* on the image *i*. (x_{ijk}, y_{ijk}) are the coordinates of the point *k* placed in the image *i* on the contour of the structure *j*. From these two matrices, the shape model of each structure and the corresponding distance and orientation models can be constructed. Indeed, from two matrices of points obtained, we can calculate the mean shape relative to each structure [Ham98]:

$$\bar{V}_1 = \frac{1}{N}\sum_{i=1}^{N} v_{i1} \quad (1)$$

$$\bar{V}_2 = \frac{1}{N}\sum_{i=1}^{N} v_{i2} \quad (2)$$

Then, we can determine the modes and the amplitudes of deformation of every shape by applying the PCA on aligned shapes. Each structure can be represented by a shape model that describes its geometry and deformation modes. These models can be respectively defined by Equations (3) and (4). They represent a priori knowledge of shape of each structure.

$$V_1 = \bar{V}_1 + P_1 b_1, \quad (3)$$

$$V_2 = \bar{V}_2 + P_2 b_2, \quad (4)$$

With: P_1 and P_2 are respectively the matrices of the main deformation modes of the first and the second structure. b_1 and b_2 are two weight matrices which represent respectively the projection of the shape V_1 in the base P_1 and the shape V_2 in the base P_2

3.1.1 Construction of the Statistical Distance Model

The statistical distance model is made at the same time as that of the shape's models. It first consists in computing the distances between both structures of interest from the training images and then trying to deduce a compact and precise formulation, which describes the authorized distances. Given an image *i* of the training set where both structures of interest are modeled respectively by the two following vectors:

$$v_{i1} = (x_{i11}, y_{i11}, \ldots, x_{i1j}, y_{i1j}, \ldots, x_{i1n}, y_{i1n}) \quad (5)$$

$$v_{i2} = (x_{i21}, y_{i21} \ldots, x_{i2k}, y_{i2k}, \ldots, x_{i2m}, y_{i2m}) \quad (6)$$

First, we proceed to calculate the centers of gravity of two structures: $B_{i1}(Gx_{i1}, Gy_{i1})$ and $B_{i2}(Gx_{i2}, Gy_{i2})$. For example, the calculation of center of gravity of a structure modeled by a vector v_{i1} is as follows [Bou88]:

• Surface of the structure:

$$A = \frac{1}{2}\sum_{i=0}^{n-1}(x_i y_{i+1} - x_{i+1} y_i) \quad (7)$$

• Coordinates of center of gravity:

$$G_x = \frac{1}{6A}\sum_{i=0}^{n-1}(x_i + x_{i+1})(x_i y_{i+1} - x_{i+1} y_i) \quad (8)$$

$$G_y = \frac{1}{6A}\sum_{i=0}^{n-1}(y_i + y_{i+1})(x_i y_{i+1} - x_{i+1} y_i) \quad (9)$$

Then, the Euclidean distance between B_{i1} and B_{i2} is defined by:

$$d(B_{i1}, B_{i2}) = \sqrt{(Gx_{i1} - Gx_{i2})^2 + (Gy_{i1} - Gy_{i2})^2} \quad (10)$$

Therefore, the elementary distance d_i between the two structures of interest in an image *i* can be defined by:

$$d_i(v_{i1}, v_{i2}) = d_i(v_{i2}, v_{i1}) = d(B_{i1}, B_{i2}) \quad (11)$$

With the same principle, we can calculate the distances between the two structures of interest through all the images of the training set. Thereby obtaining a vector of distances of dimension *N*:

$$v_d = (d_1, d_2, \ldots, d_i, \ldots, d_N) \quad (12)$$

The objective now is to deduce a compact formulation that describes authorized distances. Indeed, from the vector v_d, we can calculate the following basic statistical parameters:

- The mean distance between two structures of interest:

$$d_m = \frac{1}{N}\sum_{i=1}^{N} d_i \quad (13)$$

- The variance which measures the dispersion of elementary distances d_i around the mean distance:

$$V(v_d) = \frac{1}{N} \sum_{i=1}^{N} (d_i - d_m)^2 \quad (14)$$

- The standard deviation, which represents the mean of all the elementary distances around the mean distance:

$$\sigma = \sqrt{V(v_d)} \quad (15)$$

- The confidence interval around the mean distance can be defined using these parameters. This interval includes a large percentage of the initial elementary distances. Usually, the most adopted degree of confidence is equal to 95.4%. This degree leads to a confidence interval, limited as follows:

$$[d_m - 2\sigma,\ d_m + 2\sigma] \quad (16)$$

This means that if we consider a new image to be segmented, the distance between both structures of interest belongs to the interval at 95.4%. A compact formulation of the distance between structures can be defined by:

$$d = d_m + 2\varphi\sigma, \quad (17)$$

With φ is a real parameter in the interval $[-1, 1]$. The Equation 17 defines then the statistical distance model. This model represents thus a priori knowledge based on the variation of the distance between structures. It can be effectively used in the localization phase, to constrain the evolution of the initial shapes. For that purpose, we should calculate at each iteration, the parameter φ as a function of the current distance d_c (distance between the two shapes in the current iteration). Defined as follows:

$$\varphi = \frac{d_c - d_m}{2\sigma} \quad (18)$$

There are then three possible cases:

$$\begin{cases} \text{If } \varphi \in [-1,1] \text{ then valid distance} \\ \quad If\ \varphi > 1 \text{ then } \varphi \leftarrow 1 \\ \quad If\ \varphi < -1 \text{ then } \varphi \leftarrow -1 \end{cases} \quad (19)$$

In this way, we can require that the distance between shapes will always be in the authorized interval.

3.1.2 Construction of the Statistical Orientation Model

Likewise, the statistical orientation model is calculated at the same time as the shapes and distance models. This model is based on the angle variation between both structures to be segment. It consists to calculate the angles between both structures from the training images and try to deduce a compact formulation, which describes the allowed angles.

First, we will calculate the centers of gravity of the studied structures B_{i1} (Gx_{i1}, Gy_{i1}) and B_{i2} (Gx_{i2}, Gy_{i2}), as described in the previous section.

Then, to calculate the angle θ between both structures (that is the angle formed by the intersection of the line passing through the two centers of gravity B_{i1} and B_{i2} and the horizontal axis *ox*, Figure 1) we proceed as follows:

$$a = \frac{Gy_{i2} - Gy_{i1}}{Gx_{i2} - Gx_{i1}} = \tan(ox, B_{1i}\, B_{2i}) = \tan\theta, \quad (20)$$

with a is the slope of the line $(B_{i1}\, B_{i2})$

$$\theta = \tan^{-1}(a) \quad (21)$$

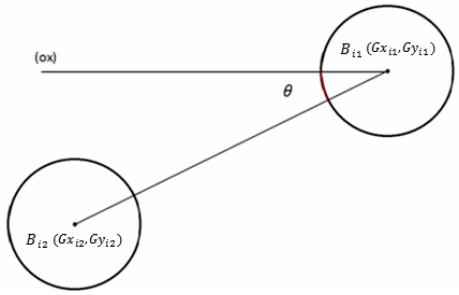

Figure 1: Representation of the angle θ between the reference object (right) and the target object (left)

Similarly, we can calculate the angles between both structures of interest through all the images of the training set. Thereby obtaining an N-dimensional vector angles:

$$v_\theta = (\theta_1, \theta_2, \dots, \theta_i, \dots, \theta_N) \quad (22)$$

The aim now is to deduce a compact formulation that describes authorized angles. Indeed, from the vector v_θ , we can calculate the following basic statistical parameters:

- The mean angle between two structures of interest:

$$\theta_m = \frac{1}{N} \sum_{i=1}^{N} \theta_i\ , \quad (23)$$

The variance which measures the dispersion of elementary angles θ_i around the mean angle:

$$V(v_\theta) = \frac{1}{N} \sum_{i=1}^{N} (\theta_i - \theta_m)^2 \quad (24)$$

- The standard deviation, which represents the mean of all the elementary angles around the mean angle:

$$\sigma_1 = \sqrt{V(v_\theta)} \quad (25)$$

The confidence interval around the mean angle can be defined using these parameters. This interval includes a large percentage of the initial elementary angles. Usually, the most adopted degree of confidence is equal to 95.4%. This degree leads to a confidence interval, limited as follows:

$$[\theta_m - 2\sigma_1,\ \theta_m + 2\sigma_1] \quad (26)$$

This means that if we consider a new image to be segmented, the angle between both structures of interest belongs to the interval at 95.4%.

Finally, a compact formulation of the angle between structures can be defined by:

$$\theta = \theta_m + 2\varphi_1\sigma_1, \quad (27)$$

With φ_1 is a real parameter in the interval $[-1, 1]$.
The Equation 27 defines then the statistical orientation model. This model represents thus a priori knowledge based on the variation of the angle between structures. It can be effectively used in the localization phase, to constrain the evolution of the initial shapes. For that purpose, we should calculate at each iteration, the parameter φ_1 as a function of the current angle θ_c (angle between both shapes in the current iteration), defined as follows:

$$\varphi_1 = \frac{\theta_c - \theta_m}{2\sigma_1} \quad (28)$$

There are then three possible cases:

$$\begin{cases} \text{If } \varphi_1 \in [-1,1] \text{ then valid angle} \\ If\ \varphi_1 > 1 \text{ then } \varphi_1 \leftarrow 1 \\ If\ \varphi_1 < -1 \text{ then } \varphi_1 \leftarrow -1 \end{cases} \quad (29)$$

In this way, we can require that the angle between shapes will always be in the authorized interval. This allows avoiding the divergence and the collision of shapes during the evolution and increasing the accuracy of results.

Segmentation Guided by Shape, Distance and Orientation Models

The segmentation procedure is sequential. Indeed, the easiest structure to be obtained is segmented first using the standard ASM. The result will then be used as a reference for the segmentation of other structures, based on a priori knowledge of shape, distance and orientation. Thus, the segmentation process can be simulated by the algorithm 1.

Algorithm 1 Segmentation guided by shape, distance and orientation models

$\bar{V}_r$: *mean_shape_reference_structure*
F_r *: Result_localisation_reference _structure*
$\bar{V}_{cibl}$ *: mean_shape_target_structure*
F_{cibl_i} *: Result_localisation _target_iteration_i*
F_{cibl_i}' *: Result_ intermediate _iteration_i*
d_c *: current Distance*
θ_c *: current Angle*
%%%%Segmentation to the reference structure
F_r=*procedure_segmentation_ASM* $(\bar{V}_r, V_r = \bar{V}_r + P_r b_r)$
%%%% Segmentation target structure
i=*0*
While (convergence==no and $i <$ *nbr_max_iterations)*
1. F_{cibl_i}' =*procedure_segmentation_ASM* $(F_{cibl\_i}, V_{cibl} = \bar{V}_{cibl} + P_{cibl} b_{cibl})$
2. d_c = *distance* (F_r, F_{cibl_i}')
3. θ_c = *angle* (F_r, F_{cibl_i}')
4. $(F_{cibl\_(i+1)})$=*limitation_distance_angle* $(d_c, \theta_c, F_r, F'_{cibl\_i}, d = d_m + 2\varphi\sigma, \theta = \theta_m + 2\varphi_1\sigma_1)$
5. *Convergence=compare* $(F_{cibl\_i}, F_{cibl\_(i+1)})$
6. *i=i+1*

End

The limitation by distance and orientation constraint can be simulated by algorithm 2.

Algorithm 2 limitation by distance and orientation constraint

v, w *: real variables*
F_x *: coordinate of the target shape,* F_y *: ordinate of the target shape,* F'_x*: new coordinate of the target shape,* F'_y*: n ordinate of the target shape*
d_m *: mean distance,* σ *: standard deviation_distance,* d_c *: current distance,* φ *: real parameter_distance,* d_{min} *: minimum distance,* d_{max} *: maximum distance*
θ_m *: mean angle,* σ_1 *: standard deviation_angle,* θ_c*: current angle,* φ_1 *:real parameter_angle,* θ_{min} *: minimum angle,* θ_{max} *: maximum angle*

If $\varphi < -1$ *then #* $(d_c < d_{min})$
$v = d_{min} - d_c$
If $\varphi_1 < -1$ *then #* $(\theta_c < \theta_{min})$
$w = \theta_{min} - \theta_c$
$F'_x = F_x cos(w) - F_y sin(w) - v$
$F'_y = F_x sin(w) + F_y cos(w) - v$
If $\varphi_1 > 1$ *then #* $(\theta_c > \theta_{max})$
$w = \theta_c - \theta_{max}$
$F'_x = F_x cos(w) + F_y sin(w) - v$
$F'_y = -F_x sin(w) + F_y cos(w) - v$
Else
$F'_x = F_x - v$
$F'_y = F_y - v$

If $\varphi > 1$ *then #* $(d_c > d_{max})$
$v = d_c - d_{max}$
If $\varphi_1 < -1$ *then #* $(\theta_c < \theta_{min})$
$w = \theta_{min} - \theta_c$
$F'_x = F_x cos(w) - F_y sin(w) + v$
$F'_y = F_x sin(w) + F_y cos(w) + v$
If $\varphi_1 > 1$ *then #* $(\theta_c > \theta_{max})$
$w = \theta_c - \theta_{max}$
$F'_x = F_x cos(w) + F_y sin(w) + v$
$F'_y = -F_x sin(w) + F_y cos(w) + v$
Else
$F'_x = F_x + v$
$F'_y = F_y + v$

Else
If $\varphi_1 < -1$ *then #* $(\theta_c < \theta_{min})$
$w = \theta_{min} - \theta_c$

$$F'_x = F_x\,cos(w) - F_y\,sin(w)$$
$$F'_y = F_x\,sin(w) + F_y\,cos(w)$$
If $\varphi_1 > 1$ *then* $\#(\theta_c > \theta_{max})$
$w = \theta_c - \theta_{max}$
$$F'_x = F_x\,cos(w) + F_y\,sin(w)$$
$$F'_y = -F_x\,sin(w) + F_y\,cos(w)$$
Else
$$F'_x = F_x$$
$$F'_y = F_y$$
End
End
End

4. APPLICATION TO STRIATUM SEGMENTATION IN MRI

The striatum is a nervous subcortical structure which consists of the caudate nucleus and putamen. It is a pair structure. This structure is responsible for many functions such as the execution of our movements (voluntary or automatic) and pain management. It is involved in several neurological diseases including Huntington's disease which causes the degeneration of neurons in the striatum in the first place, causing a strongly disturbed motility. In clinical practice, an early diagnosis of Huntington's disease is based, necessarily, on the detection of atrophy of striatum structures. Many segmentation methods have been proposed to contribute to the quantification of striatum atrophy. These models are derived from a statistical learning database [Yan04]. Other works are based on deformable models [Col04]. In [Bab08], the authors present an interesting qualitative and quantitative comparison of the four methods [Alj07, Bab07, Mur07, Pat07] applied for segmentation of internal brain structures on the MRI images, including the caudate nucleus and putamen. The difficulties faced in these applications come mainly from poor definition of these anatomical structures and boundaries. The extraction of these structures is thus often a laborious task.

In this context, we propose a contribution to segment internal brain structures, particularly the caudate nucleus and putamen based on three types of statistical a priori knowledge: the shape of each structure, the distance and the orientation variability between them.

Training step

To model the shapes of the studied structures, we used a training set of 40 brain MRI images (size 256 * 256) from ten different volumes. From each volume, we selected four T1-weighted axial images with the target structures. Then, a labeling step is applied to extract the shapes of both structures: 14 points are used to extract the caudate nucleus and 16 points to extract the putamen.

In the training step, the variability percentage of the original data is fixed at 95% and the length of the grey levels profile is 7 pixels.

As a result, we ended up building a shape model for each structure (the reference structure is presented by the caudate nucleus and the target structure is presented by the putamen), a distance model and an orientation model, which describes the variation of the distance and the angle between them. The parameters of the obtained models are shown in Table 1.

	Caudate nucleus	**Putamen**
Shapes models	5 principal variation modes	3 principal variation modes
Distance model	Mean distance $d_m = 19.57$ standard deviation_distance $\sigma = 1.66$	
Orientation model	Mean angle $\theta_m = 50.64$ standard deviation_angle $\sigma_1 = 3.34$	

Table 1: Parameters of shapes models, distance model and orientation model

Segmentation Step

The segmentation procedure is sequential. First, we start with the segmentation of the reference structure based only on the original model (ASM). In this application, after series of tests, we chose the caudate nucleus as a reference structure (the simplest structure to segment). The initialization is the mean shape of the caudate nucleus obtained during training step (figure2.intialization). The segmentation result is illustrated by following figure:

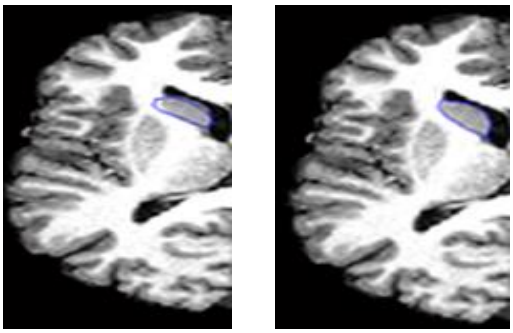

Initialization **Segmentation result**

Figure 2: Segmentation of the reference structure (caudate nucleus) with ASM

Then, we proceed to the putamen segmentation, based on the ASM and spatial relations "ASM+SR". In the various tests, the used initializations are calculated, each time, according to the mean shapes of the putamen obtained during the training step. The maximum number of iterations is set to 60 iterations and the length of the search profile is equal to 21 pixels. In the following, figure 3 shows an example of the segmentation result of the putamen based on ASM+SR, with a good initialization.

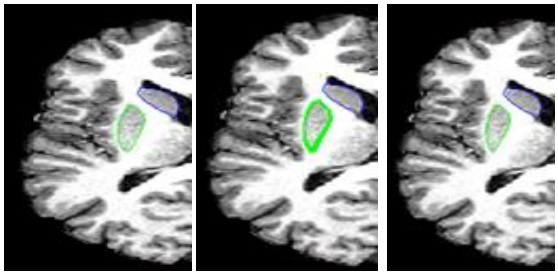

(a) (b) (c)

Figure 3: segmentation of the putamen based on ASM+SR. (a) initialization of the mean shape. (b) deformation of the contour. (c) final segmentation result

It is observed that the evolution is performed at a very close neighbor of the target structure. This can provide information on the positive impact of a priori knowledge (shape, distance and orientation) used in the segmentation process.

Qualitative evolution

In order to study the behavior of the curve in the evolution process, with and without the constraint of spatial relations, we made a comparison between the proposed method ASM+SR and the original model ASM. The comparison is performed, in each case, on the same image with the same propagation conditions and by adopting different initializations:

- Case 1: close initializations

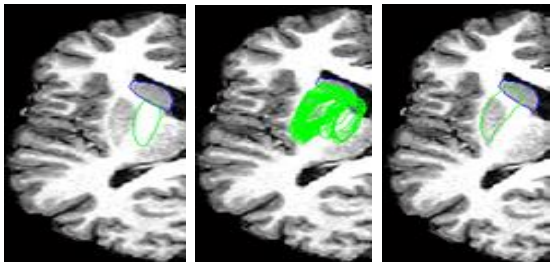

(a)

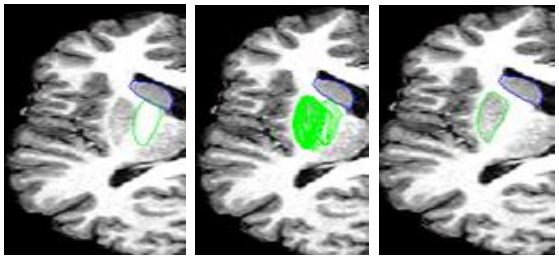

(b)

Figure 4: Examples of obtained results with close initializations. The first column shows the initializations, the second column shows the deformation of the contour and the third column shows corresponding results. (a) Obtained result with ASM. (b) Obtained result with ASM+SR

- Case 2: far initializations

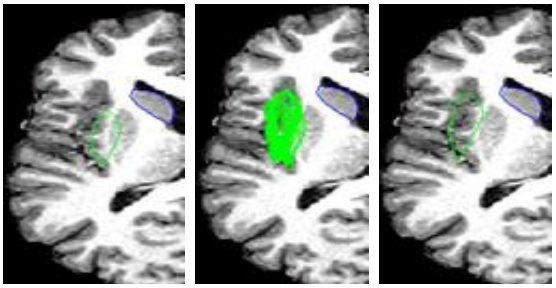

(a)

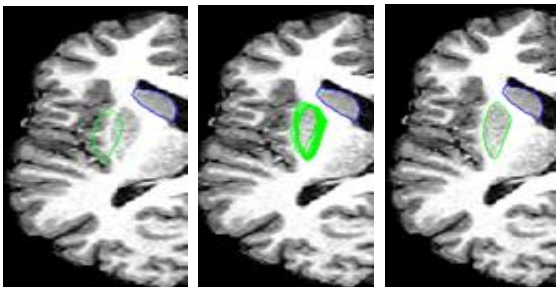

(b)

Figure 5: Examples of obtained results with far initializations. The first column shows the initializations, the second column shows the deformation of the contour and the third column shows corresponding results. (a) Obtained result with ASM. (b) Obtained result with ASM+SR

Looking at figure 4.a, we can see that if the initialization of the putamen is close to the reference structure, and using original model ASM, the final shape cannot properly define the target structure. There is also a collision between the results. However, in figure 4.b, using the ASM+RS (assuming of course the same initialization), we find that the final shape correctly converged towards the target structure. We can also observe that during evolution, the application of spatial relations make shape gradually pushed towards the target structure. What explains the significant difference between the accuracy of the final result by the ASM+RS and that obtained by ignoring the spatial constraints.

Similarly, by examining figure 5.a and figure 5.b, we see that when ignoring spatial constraints, the final shape diverges to an area where the image intensity is similar to that of Putamen. But the use of spatial constraints helped to push the shape to the target structure and thus obtain a satisfactory result.

In conclusion, these results can provide information on the positive contribution of integrated spatial relationships. Indeed, the application of spatial constraints (distance and orientation) during the evolution has limited the distortion of the initial shape in an authorized zone and thus prevents the divergence to neighboring areas of similar intensity.

However, it must be said that these results can be enhanced to include more examples in the validation process. We must also think about a quantitative evolution in these results

5. CONCLUSION

We have attempted to validate the proposed model "ASM+RS" on a clinical application: segmentation of the caudate nucleus and putamen in MRI cuts of the brain. The obtained results are promising and show good performance of the proposed model. Indeed, the use of an additional constraint of spatial relations (distance and orientation) in the localization step can constrain the development in the regions of interest and achieve satisfactory results. In most of the tests, the proposed model showed its robustness and stability. However, there are limits and a number of perspectives. Indeed, we have not managed to test our model on pathological subjects, thus the precise quantification of the studied pathologies remains incomplete. This is due to the lack of sufficient data in the problem studied. In addition, we treated the case of segmentation of two objects and the proposed method can be easily extended to locate n structures, which will be addressed in future work. Moreover, this method can be improved by adding other spatial constraints to the active shape model e.g., symmetry, which is an important feature of the medical images.

6. REFERENCES

[Alj07] Aljabar, P., Heckemann, R., Hammers, A., Hajnal, J. and Rueckert, D. Classifier selection strategies for label fusion using large atlas databases, MICCAI 2007.

[Bab07] Babalola, K. O., Petrovic, V., Cootes, T. F., Taylor, J. C., Twining, J. C., Williams, T. G. and Mills, A. Automated segmentation of the caudate nuclei using active appearance models. In 3D Segmentation in the clinic: A grand challenge. Workshop Proceedings, MICCAI 2007.

[Bab08] Babalola, K. O., Patenaude, B., Aljabar, P., Schnabel, J., Kennedy, D., Crum, W., Smith, S., Cootes, T. F., Jenkinson, M. and Rueckert, D. Comparison and Evaluation of Segmentation Techniques for Subcortical Structures in Brain MRI. MICCAI, 2008.

[Bar15] Barhoumi, W., Khlifa, N. and Abidi, M. Integration of a Fuzzy Spatial Constraint into Active Shape Models for ROI Detection in Medical Images Current Medical Imaging Reviews. Vol. 11, No. 1, 2015.

[Bou88] Bourke, P. Calculating the Area and Centroid of a Polygon. July 1988

[Col04] Colliot, O. Représentation, évaluation et utilisation de relations spatiales pour l'interprétation d'images. Application à la reconnaissance de structures anatomiques en imagerie médicale, 2004.

[Coo95] Cootes, T.F., Taylor, C.J., Cooper, D.H., and Graham, J. Active Shape Models Their Training and Application. Computer Vision and Image Understanding, vol.6, pp.38-59, 1995.

[Ett14] Ettaieb, S., Hamrouni, K. and Ruan, S. Statistical models of shape and spatial relation-application to hippocampus segmentation. 9th International Conference on Computer Vision Theory and Applications, Lisbon-Portugal, 2014.

[Fou10] Fouquier, G. Doctorat, Ecole Nationale Supérieure des Télécommunications, 2010.

[Gér00] Géraud, T.H. Reconnaissance de structures cérébrales à l'aide d'un atlas et par fusion d'informations structurelles floues, 12 ème Congrès Francophone AFRIF-AFIA de Reconnaissance des Formes et Intelligence Artificielle (RFIA'2000). Vol.1, pp.287-295, Paris- France, Février 2000.

[Ham98] Hamarneh, G. Active Shape Models - Part I: Modelling Shape and Gray Level Variations. Proceedings of the Swedish Symposium on Image Analysis, 1998.

[Hud08] Hudelot, C., Atif, J. and Bloch, I. FSRO : une ontologie de relations spatiales floues pour l'interprétation d'images, Revue des Nouvelles Technologies de l'Information-les Relations Spatiales : de la Modélisation à la mise en œuvre. RNTI-E-14, pp.53-84, 2008.

[Jaa11] Jaafar, B. and Khlifa, N. Conception of a 2D active-shape model integrating a spatial relation card based on a fuzzy logic. Proceedings of International Conference on Communications, Computing and Control Applications. Hammamet, Tunisia, 2011.

[Kas87] Kass, M., Witkin, A. and Terzopoulos, D. Snakes: Active contour models. International Journal of Computer Vision, 1(4) 321–331, 1987.

[Mur07] Murgasova, M., Dyet, L., Edwards, A. D., Rutherford, M., Hajnal, J. and Rueckert, D. Segmentation of brain MRI in young children. Acad. Rad, 2007.

[Nem09] Nempont, O. Modèles structurels flous et propagation de contraintes pour la segmentation et la reconnaissance d'objets dans les images. Application aux structures normales et pathologiques du cerveau en IRM, Mars 2009.

[Pat07] Patenaude, B., Smith, S., Kennedy, D. and Jenkinson, M. Bayesian shape and appearance models. Technical report TR07BP1, FMRIB Centre - University of Oxford, 2007.

[Per02] Perchant, A. and Bloch, I. Fuzzy Morphisms between Graphs. Fuzzy Sets and Systems. vol.128, pp.149–168, 2002.

[Yan04] Yang, J., Staib, L. H. and Duncan, J. S. Neighbor-Constrained Segmentation With Level Set Based 3-D Deformable Models. IEEE TMI, vol.23, pp.940-948, 2004.